International Journal of Nanoscience
Vol. 22, No. 2 (2023) 2350014 (6 pages)

DOI: 10.1142/S0219581X2350014X

World Scientific
www.worldscientific.com

Effect of Molar Concentration and Solvent Type on Linear and NLO Properties of Aurintricarboxylic (ATA) Organic Dye for Image Sensor and Optical Limiter Applications

Anwar Ahmed Fadhl Abodood*, Karar Abdali†, Abdulazees O. Mousa Al-Ogaili‡,¶, Ehssan Al-Bermany§ and Khalid Haneen Abass§

*College of Medical and Health Technologies
Al-Zahraa University for Women, Karbala, Iraq

†Iraq, Ministry of Education

‡Department of Physics, College of Science
University of Babylon
Al Hillah, Babylon, Iraq

§Department of Physics
College of Education for Pure Science
University of Babylon, Al Hillah, Babylon, Iraq

¶aaazezphys@gmail.com

Received 28 November 2022
Accepted 9 January 2023
Published 18 February 2023

Aurintricarboxylic (ATA) organic dye is a promising chemical compound candidate for several optical and electronic applications. However, this study aims to investigate the impact of molar concentrations and solvent type on the linear/nonlinear optical (NLO) properties of 5,5′-[(3-carboxy-4-oxocyclohexa-2,5-dien-1-ylidene) methylene] bis (2-hydroxybenzoic acid) organic laser dyes. Three molar concentrations of organic dyes (2×10^{-3}, 4×10^{-3}, and 6×10^{-3}) M were respectively dissolved in distilled water and dimethylsulfoxide (DMSO) at room temperature. The samples were investigated using ^{1}H-NMR and UV/Visible spectrums. The bandgap (E_g) of (2×10^{-3} M) ATA/water is 4.75 eV, but Eg of ATA/DMSO was 2.93 eV and 2.65 eV. The measurements were performed by employing a diode-pumped solid-state laser operating at a 457 nm wavelength and 112 mW of power. The Z-scan technique was applied to characterize open and close apertures, nonlinear refractive index (n), and nonlinear absorption coefficient (β). The obtained results predicted that both the n and β coefficients decreased with the reduction of molar concentrations. Additionally, DMSO exhibited better linear/NLO properties than water. The results revealed promising laser dye samples for image sensor and optical limiter applications.

Keywords: ATA; optical properties; Z-scan technique; optical limiter.

1. Introduction

ATA dye has recently been viewed as a promising candidate owing to its optical, electronic, and industrial advancements.[1] Organic dyes are fluorescent molecules with large molecular weights and are characterized by their containing extended systems of conjugated double bonds. In a dye laser, these molecules are dissolved in an organic solvent or incorporated into a solid matrix. They usually have a strong absorption band in the range between the ultraviolet and the near-infrared. Although dyes have been demonstrated to laser in the solid, liquid, or gas phase, it is in the liquid and solid phases that dyes have made a significant impact as laser media.[1] Solid-state dye lasers span from the UV to the near-IR regions. An important feature of the dye laser is that it is easily tunable over a wide range of wavelengths. The use of solutions in dye lasers entails several liquid inconveniences, which are mainly large volumes of organic dye solutions, which are toxic and expensive. Through the incorporation of dye molecules into solid matrices, attempts were made to overcome the problems posed by dye solutions. This revealed significant advances toward the development of practical tunable solid-state lasers.[2] Because of their high fluorescence quantum yield and broad gain bandwidth, organic dyes have a wide range of applications in scientific research.[3] The wide bandwidth makes them suitable for tunable ultrafast pulse generation. Due to the wide range of uses in various electronic applications, the study of the electrical properties of dyes is very important nowadays, but there are different factors that affect the behavior of studying samples, such as sintering temperature, which must be studied.[4] This work aims to investigate the effects of molar concentration and solvent type on the linear and NLO properties of the ATA organic dye.

2. Experimental Section

2.1. *Materials*

ATA powder was purchased from Aldrich with a (300–302)°C melting point and a 473 molecular weight.

2.2. *Characterizations and procedures*

The UV/Visible absorbance was measured using a Shimadzu spectrometer with wavelength range of (190–1100) nm. The NLO properties were measured using the Z-scan technique via a diode-pumped solid-state laser operating at a 457 nm wavelength and 112 mW of power. The LASER beam waist is 0.025 cm and the movement steps size is 0.5 mm. To focus the laser beam on the sample, the convex lens with a focal length of 15 cm was used. The specimens were excited for the laser beam at normal incidence geometry. The specimen was shifted back and forth along the z-axis around the minimum beam waist of the laser during the Z-scan calculation in order to measure transmittance as a function of the sample location.

2.3. *Synthesis method*

The ATA dye was prepared based on the literature.[5,6] In brief, 10 g (0.014 mol) of solid potassium nitrate was constructed in 70 mL of sulphuric acid using a stirrer for 2 h, and then 20 g (0.014 mol) of salicylic acid was added to the mixture and stirred continuously for 0.5 h. The mixture was placed in the ice-salt bath to control the mixture temperature at room temperature. Until the mixture presented a light red to brown color, 1.95 g (0.065 mol) of formaldehyde was slowly added with extremely vigorous stirring, followed by 100 g of crushed ice. The stirring should be vigorous during the addition. The contents of the flask are stirred until the ATA has disintegrated into small pieces. The chemical structure of ATA dye is 5,5′-[(3-carboxy-4-oxocyclohexa-2,5-dien-1-ylidene) methylene] bis (2-hydroxybenzoic acid), as shown in Fig. 1. A ^{1}H-NMR spectrum was recorded using Bruker-AV500 at 500 MHz for ^{1}H. Chemical shifts d are reported in ppm relative to TMS and coupling constants J are in Hz and have been rounded to the nearest whole number. Assignments of signals are based on integration values, coupling patterns, and expected chemical shift values and have not been rigorously confirmed. The resulted dye had M.P= (300–302)°C, IR (v, cm^{-1}): 3400–2990 (OH), 1707 (C=O), 1602 (ph = O), 2987,2848 (C–H aliph),

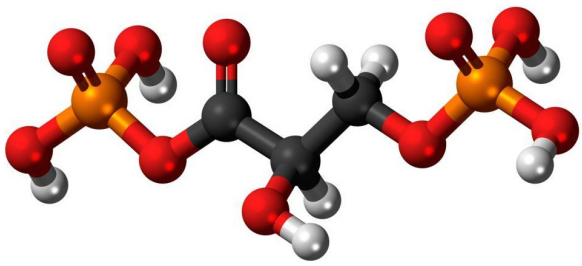

Fig. 1. The 3D structure formula of ATA.[7]

3118 and 2891 (aromatic CH), 1H-NMR (d-DMSO) (ppm): 5.35 (s, 2 H, OH), 6.40 (d, 2H, ph-H), 7.10–7.50 (d, 6H, Ar-H), 8.10 (d, 1H, ph-H), 11.0 (s, 3H, carboxyl OH).[5,6]

2.4. *Theoretical calculations*

Three concentrations of organic ATA dye solution in distilled water and DMSO solvents (2×10^{-3}, 4×10^{-3}, and 6×10^{-3}) M were prepared using the following equation:[8,9]

$$W = \frac{M_w \times V \times C}{1000}, \tag{1}$$

where W is the weight of the dissolved dye, M_w is the molecular weight of the dye, V is the volume of the solvent, and C is the dye concentration.

The prepared solution was diluted according to the following equation:[10]

$$C1 \cdot V1 = C2 \cdot V2, \tag{2}$$

where $C1$ and $C2$ are primary and secondary concentrations, and $V1$ and $V2$ are the volumes before and after dilution.

3. Results and Discussion

The NLO properties of the sample in different concentrations (2×10^{-3}, 4×10^{-3}, and 6×10^{-3}) M using a continuous wave (CW) diode pump solid-state blue laser at the wavelength 457 nm and 112 mW power were investigated. The NLO properties were measured in the open and closed-aperture Z-scan cases.

3.1. *The linear optical properties*

Herein, two solvents were used: distilled water and DMSO. DMSO is an organosulfur compound with the formula $(CH_3)_2SO$. DMSO is a dipolar aprotic solvent that dissolves both polar and nonpolar compounds and is miscible in a wide range of organic solvents as well as water. It has a relatively high melting point. In terms of chemical structure, the molecule has idealized symmetry. It has a trigonal-pyramidal molecular geometry, similar to other three-coordinate compounds, and a nonbonded electron pair on the roughly tetrahedral sulfur atom. DMSO has a low level of toxicity.[5] As shown in Fig. 1, The absorbance of DMSO + ATA is greater than the absorbance of water + ATA, due to the presence of the carboxyl group (COOH) and hydroxyl group (–OH) in the ATA structure that assist it to forms the H bonds with symmetric molecules or with water molecules and then decreasing the absorbance. Although water has a very polar O–H bond, DMSO also has a very polar S–O bond. The electronic transition between S and O is a major reason for increasing the electrical conductivity and decreasing the bandgap.[6,8] Then, ATA in distilled water has low absorbance and high Eg compared with the ATA in DMSO. The linear absorbance and E_g of (2×10^{-3}) M ATA in the water and DMSO solvents were shown in Fig. 2.

3.2. *The nonlinear absorption coefficient*

The nonlinear absorption coefficient of an investigated organic dye with different molar concentrations in distilled water and DMSO solvents was

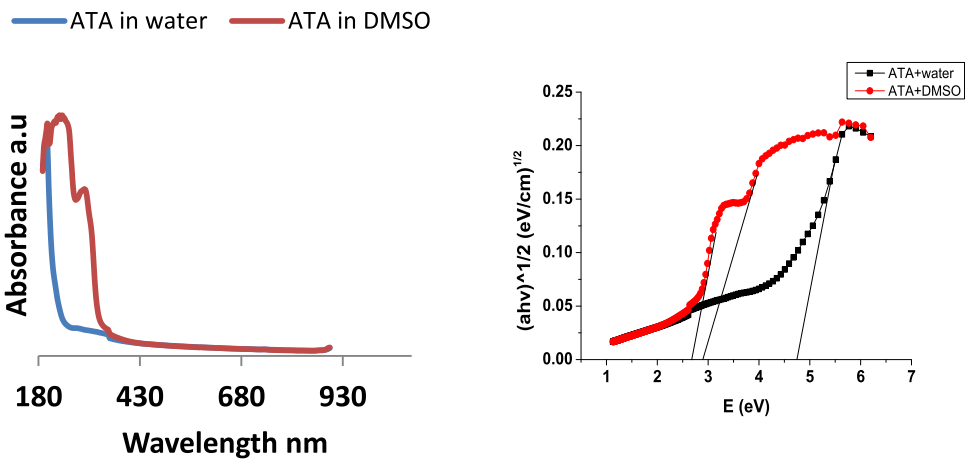

Fig. 2. The linear optical characterization of ATA in water and DMSO solvent.

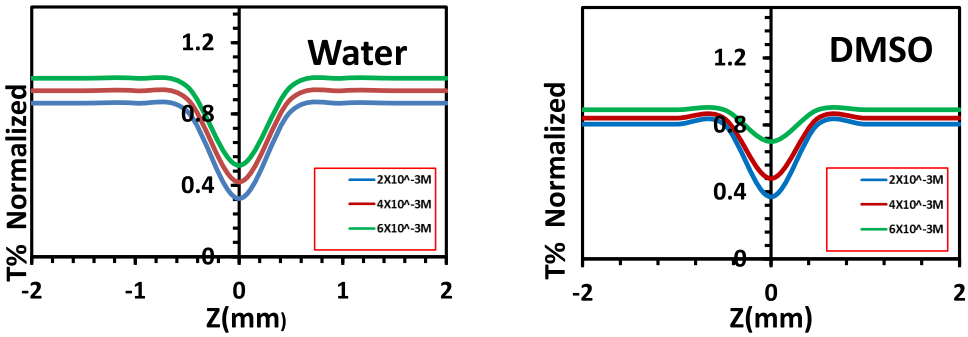

Fig. 3. Open-aperture Z-scan data of ATA compound in distilled water and DMSO.

measured by the open-aperture Z-scan technique. They performed an open-aperture Z-scan that exhibited an improvement in the transmission of the focus of the lens. Open-aperture Z-scan of the sample at (457 nm) (112 mW) in both solvents, as shown in Fig. 3, which exhibited the two-photon absorption phenomenon. The behavior of transmittance starts linearly at different distances from the far field of the sample position (−Z). At the near field, the transmittance curve begins to decrease until it reaches the minimum value (T min) at the focal point, where Z = 0 mm. At the far-field of the sample position (+Z), the transmittance begins to increase towards linear behavior. change of intensity was caused by two-photon absorption when the sample travels through the beam waist. The open-aperture Z-scan defines variable transmittance values, which were used to determine the absorption coefficient. This behavior is consistent with other findings.[5,11]

3.3. *The nonlinear refractive index*

The nonlinear refractive index of the prepared dye samples in different concentrations (distilled water and DMSO solvents) was measured by the closed-aperture Z-scan technique. The normalized transmittances of Z-scan measurements as a function of the distance between both solvents are shown in Fig. 4. The nonlinear effect region was extended from (−1.5 to 1.5) mm. The peak is followed by a valley transmittance curve obtained from the closed aperture Z-scan data that indicates the sign of the refraction nonlinearity was positive ($n_2 > 0$) and led to self-focusing lensing of this sample.[12] The Z-scan behavior is described as moving the sample far from the focus. Here the transmitted beam intensity is low and the transmittance remains relatively constant. As the sample approaches the beam focus, the intensity increases, leading to self-lensing in the sample that tends to collimate the beam on the aperture in the far field and increase the measured transmittance at the position. If the beam finds any nonlinear phase shift through the sample, that will translate through the focal region, then the fraction of light falling on the detector will vary via the self-lensing generated in the material by the intense laser beam. In this case, the signal measured by the detector will exhibit a peak and valley as the sample is transmitted. The position of the peak and valley is relative to the z-axis, which depends on the sign of the nonlinear

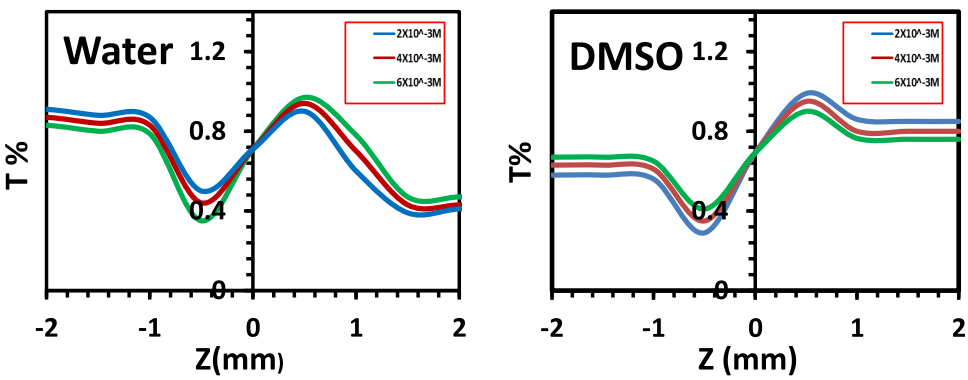

Fig. 4. Closed-aperture Z-scan data of ATA compound in distilled water and DMSO solvents.

phase shift. Where the change in normalized transmittance from the curve's peak to the valley $(T) - (p - v)$ is proportional to the nonlinear phase shift imparted on the beam. Moreover, if the beam is transmitted through the nonlinear medium, the induced phase shift can also be either negative or positive depending on the medium if it is self-focusing or self-defocusing, respectively.[13] The magnitude of the phase shift can be determined by the change in transmittance between the peak and valley. The self-defocusing increased the beam divergence, leading to a widening of the beam at the focus and reducing the measured transmittance. Because the transmittance is outside Riley range far from focus (Z $>$ 0), the nonlinear refraction was low, resulting in a transmittance Z-independent. The general behavior in the open case of the prepared samples as the solution was two-photon absorption, whereas the general behavior in the closed case of the prepared samples was self-focusing. This behavior agrees with the literature.[5,14]

The nonlinear parameters were theoretically calculated, as exhibited in Tables 1 and 2. These tables showed the values of the nonlinear parameter n2 improved with the increase of molar concentrations and β enhanced when the concentrations rose and increased the values of linear parameters (no and αo). This is associated with the increasing number of molecules per volume unit at low concentrations. The closed-aperture Z-scan defines variable transmittance values, which are used to determine the nonlinear phase shift $\Delta\Phi$o. The nonlinearity of samples dissolved in distilled water and DMSO solvents is larger, as included in Refs. 15 and 16.

3.4. *Optical limiting behavior*

The optical limiting behavior was performed by closed-aperture Z-scan with the same laser used in the Z-scan technique. Figure 5 shows the optical limiting characteristics at room temperature for the prepared sample in distilled water and DMSO solvents. The samples revealed good optical limiting behavior arising from nonlinear refraction. The output power rises initially with the increase of input power,[17–21] but after a certain threshold value, the sample starts defocusing the beam,

Table 1. The linear and NLO parameters in different concentrations by distilled water at $\lambda = 457$ nm.

C (M)	T	$(\alpha_\circ)\,\mathrm{cm}^{-1}$	$n_\circ$	ΔT_{P-V}	$n_2 \times 10^{-11}\,\mathrm{cm}^2/\mathrm{mW}$	T (z)	$\beta \times 10^{-3}$ cm/mW
2×10^{-3}	0.9925	0.0074	1.1303	0.6908	9.7623	0.7940	0.1903
4×10^{-3}	0.1531	0.1531	1.7641	0.6105	7.9645	0.8178	0.7898
6×10^{-3}	0.8212	0.1969	1.9123	0.4725	6.0019	0.8509	0.8986

Table 2. The linear and NLO parameters in different concentrations by DMSO at $\lambda = 457$ nm.

C (M)	T	$(\alpha_\circ)\,\mathrm{cm}^{-1}$	$n_\circ$	ΔT_{P-V}	$n_2 \times 10^{-11}$ cm^2/mW	T (z)	$\beta \times 10^{-3}$ cm/mW
2×10^{-3}	0.8472	0.1658	1.8074	0.5983	10.6951	0.6331	0.0947
4×10^{-3}	0.7524	0.2844	2.2139	0.5227	8.3936	0.6970	0.1280
6×10^{-3}	0.7366	0.3062	2.2776	0.4704	5.9037	0.7492	0.1901

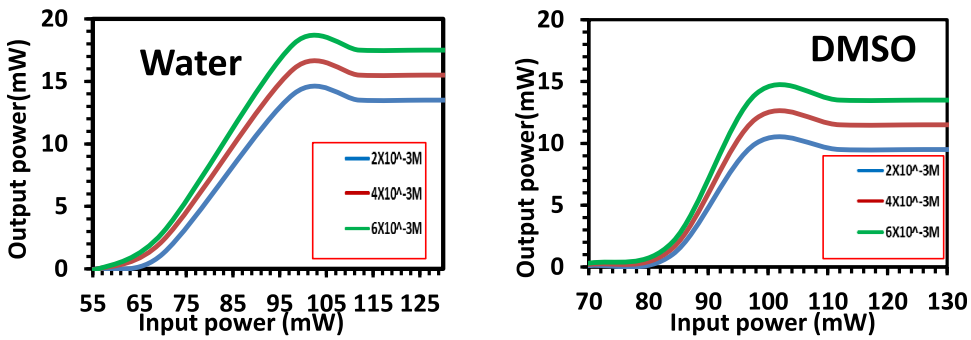

Fig. 5. The optical limiting response of ATA compound in distilled water and DMSO.

resulting in a greater part of the beam cross-section being cut off by the aperture.[21–25] Thus, the transmittance recorded by the photodetector remained reasonably constant, showing a plateau region.[22–28]

4. Conclusions

Three different molar concentrations (2×10^{-3}, 4×10^{-3}, and 6×10^{-3}) M of ATA organic dye solution in distilled water and DMSO solvents were successfully prepared. The linear optical characterizations show that the ATA in distilled water has low absorbance and high Eg compared with the ATA in DMSO. The NLO properties were investigated by the Z-scan technique in the open and closed aperture cases. The NLO properties such as β and n_2 increased with the increase in molar concentration. The distilled water solvent enhances the NLO properties more than DMSO. The optical limiting behavior was performed by closed-aperture Z-scan. The samples show good optical limiting behavior. The results suggest this dye could be used as a laser-active medium or for optical limiting applications.

References

1. S. Zafar and M. Shahid Khan, *Emerging Trends in Nanotechnology*, ed. Z. H. Khan (Springer, Singapore, 2021), doi: 10.1007/978-981-15-9904-0_13.
2. M. El-Zaidia, H. Ali, T. A. Hamdalla, A. Darwish and A. Hanafy, *Opt. Mater.* **100**, 109661 (2020).
3. M. H. Anandalli, R. F. Bhajantri, S. R. Maidur and P. S. Patil, *J. Mater. Sci. Mater. Electron.* **31**, 10531 (2020).
4. W. Hizi, H. Rahmouni, N. E. Gorji, A. Guesmi, N. Ben Hamadi, L. Khezami, E. Dhahri, K. Khirouni and M. Gassoumi, *Mangan. Catal.* **12**, 340 (2022), doi: 10.3390/catal12030340.
5. N. Al-Huda Al-Aaraji, A. O. Mousa and B. A. Naser, *IOP Conf. Ser. J. Phys. Conf. Ser.* **1234** (2019).
6. S. A. Markarian and G. A. Shahinyan, *Spectrochim. Acta A Mol. Biomol. Spectrosc.* **151**, 662 (2015).
7. B. Valuer, *Molecular Fluorescence Principles and Applications* (Wiley, New York, 2001).
8. M. Refat, A. Sedayo, A. Sayqal, A. Alharbi, H. Katouah, H. Abumelha, S. Alzahrani, F. Alkhatib, I. Athagafi and N. El-Metwaly, *Inorg. Chem. Commun.* **126**, 108472 (2021).
9. M. Fontalvo, A. Garcia, S. Valbuena and F. Racedo, *J. Phys. Conf. Ser.* **687**, 012100 (2016).
10. K. Abdali, *Silicon* **14**, 9111 (2022), doi: 10.1007/s12633-022-01678-8.
11. S. Erbaş, U. Uregil, S. Gülle and S. Baştürk, *J. Mater. Res. Expr.* **7**, 1 (2020).
12. A. Al-Khalaf, K. Abdali, A. Mousa and M. Zghair, *Asian J Chem.* **31**, 393 (2019).
13. A. Al-Zuhairi, A. Allw, K. Abdali, S. Rasool, A. Mousa, *J. Eng. Appl. Sci.* **12**, 7800 (2017).
14. H. Khalid and H. Anas, *J. Green Eng.* **10**, 4166 (2020).
15. A. Karar, F. Lamis, A. Alhak, O. Abdulazeez and A. Ali, *J. Glob. Pharma Technol.* **10**, 75 (2018).
16. K. Abdali, *Trans. Electr. Electron. Mater.* **23**, 563 (2022), doi: 10.1007/s42341-022-00388-7.
17. B. Mahdi, A. Mousa and A. Al-Zuhairi, *J. Test Eng. Manag.* **83**, 10392 (2020).
18. A. M. Kadim, K. H. Abass and A. J. Alrubaie, *AIP Conf. Proc.* **2398**, 020036 (2022).
19. K. Abdali, K. Haneen Abass, E. Al-Bermany, E. M. Al-Robayi and A. M. Kadim, *Nano Biomed. Eng.* **14**, 114 (2022), doi: 10.5101/nbe.v14i2.p114-122.
20. K. Abdali, *J. Mater. Sci. Mater. Electron.* **33**, 18199 (2022), doi: 10.1007/s10854-022-08676-x.
21. D. Seth, D. Chakrabarty and N. Sarkar, *Chem. Phys. Lett.* **401**, 546 (2005).
22. O. Abdulazeez, H. Yassin and A. Ban, *Int. J. Chem. Sci.* **4**, 2601 (2016).
23. S. Ahmed Jabbar, S. Mohammed Khalil, A. Razzaq Abdulridha, E. Al-Bermany and K. Abdali, *Key Eng. Mater.* **936**, 83 (2022).
24. J. Abdul-Kareem, M. Ali and K. Abdali, *Res. Rev. Polym. J.* **6**, 48 (2015).
25. S. A. Mukheef, F. Sh. Hashim and K. H. Abass, *HIV Nurs.* **22**, 849 (2022).
26. M. A. Kadhim, E. Al-Bermany, *J. Compos. Mater.* **55**, 2793 (2021).
27. N. R. Aldulaimi and E. Al-Bermany, *J. Phys. Conf. Ser.* **1973**, 012164 (2021).
28. A. K. Al-shammari and E. Al-Bermany, *J. Phys. Conf. Ser.* **1973**, 012165 (2021).